



Molecular Crystals and Liquid Crystals

Publication details, including instructions for authors and subscription information:

<http://www.tandfonline.com/loi/gmcl20>

Bistable Switching in Photorefractive Surface Stabilized Ferroelectric Liquid Crystals

Mara Talarico^a & Attilio Golemme^a

^a Centro di Eccellenza CEMIF.CAL, Sezione INSTM della Calabria, Dipartimento di Chimica, Università della Calabria, Rende, Italy

Version of record first published: 22 Sep 2010

To cite this article: Mara Talarico & Attilio Golemme (2007): Bistable Switching in Photorefractive Surface Stabilized Ferroelectric Liquid Crystals, *Molecular Crystals and Liquid Crystals*, 465:1, 341-358

To link to this article: <http://dx.doi.org/10.1080/15421400701206204>

PLEASE SCROLL DOWN FOR ARTICLE

Full terms and conditions of use: <http://www.tandfonline.com/page/terms-and-conditions>

This article may be used for research, teaching, and private study purposes. Any substantial or systematic reproduction, redistribution, reselling, loan, sub-licensing, systematic supply, or distribution in any form to anyone is expressly forbidden.

The publisher does not give any warranty express or implied or make any representation that the contents will be complete or accurate or up to date. The accuracy of any instructions, formulae, and drug doses should be

independently verified with primary sources. The publisher shall not be liable for any loss, actions, claims, proceedings, demand, or costs or damages whatsoever or howsoever caused arising directly or indirectly in connection with or arising out of the use of this material.

Bistable Switching in Photorefractive Surface Stabilized Ferroelectric Liquid Crystals

Mara Talarico
Attilio Golemme

Centro di Eccellenza CEMIF.CAL, Sezione INSTM della Calabria,
Dipartimento di Chimica, Università della Calabria, Rende, Italy

By using a photogenerated space-charge field to reorient the spontaneous polarization, we report an approach towards the optical control of switching in a surface stabilized ferroelectric liquid crystal that exhibits two stable orientational states. The space-charge field was generated on the surfaces of the SSFLC device, by sandwiching the FLC between two photoconducting layers, or within its bulk by doping. In the second case, we observed the formation of a grating, stable at least for months, which can be easily erased and rewritten. Experiments have been done to probe its photorefractive nature.

Keywords: bistability; liquid crystals; photorefractivity; SmC*

INTRODUCTION

Over the last two decades, an increasing interest towards dynamic holographic media has been raising, because of their possible application in several optical signal processing devices. Among these materials, the photorefractive (PR) ones show extremely interesting properties, such as high optical nonlinearity at low laser power (mW) and spontaneous beam coupling [1]. Applications of the PR effect have been proposed in several areas, including dynamic holography [2] and optical data storage [3].

This work has been partially supported by MIUR under the projects “Molecular and Organic/Inorganic Hybrid Nanostructure for Photonics – FIRB 2001” and PRIN 2004. We thank Marc Radcliffe for providing us with the liquid crystal L-15278 used in this study.

Address correspondence to Attilio Golemme, Centro di Eccellenza Cemif.Cal, Sezione INSTM della Calabria, Dipartimento di Chimica, Università della Calabria, Rende, 87036, Italy. E-mail: a.golemme@unical.it

Photorefractivity is a light induced refractive index modulation which is phase shifted with respect to a light pattern. In order to characterize their properties, PR materials are typically illuminated by two coherent laser beams, which interfere to produce a spatially modulated intensity distribution. As photoconductivity is one of the basic properties of such media, more charges of both signs are generated in the regions near the light maxima. The more mobile charge carriers can diffuse and/or drift and be trapped. The trapped carriers and the less mobile charges of opposite sign, left behind in the brighter regions, give rise to an inhomogeneous space charge distribution which, in turn, induces an internal space charge field (E_{SC}). The last step of the process is the modulation of the refractive index of the material by this internal space charge field via several effects [4], such as non-linear electro optical effects and reorientational effects. It is important to highlight the existence of a phase shift between the refractive index modulation and the initial light distribution, due to the spatial derivative that appears in Poisson equation. Only PR materials exhibit such a phase shift, which can lead to an energy transfer between two incident beams. This effect, called beam coupling [5], can be used in many optical applications.

The PR materials studied up to date are inorganic and organic crystals, amorphous organics and liquid crystals. Photorefractivity in liquid crystals was first observed in nematics [6,7], but more recently photorefractivity in bulk SmC^* phases [8] and bulk [9] and dispersed SmA^* [10] phases has also been reported. Liquid crystals are extremely appealing for photorefractivity because they exhibit several orientational mechanisms through which the space charge field can modulate the refractive index. In particular, in the case of SmC^* phases such reorientational effect can be potentially fast ($\sim \mu s$) and efficient, being the result of the coupling between the space charge field and the bulk polarization of the ferroelectric liquid crystal (FLC).

In general, in all investigations of PR FLCs reported up to now, a DC field was applied to the mesophase to enhance charge photogeneration and drift mobility, both necessary in the setting up of a PR grating. However, if one considers that the photogenerated E_{SC} modulates this externally applied DC electric field only to a small extent, it is clear that the resulting reorientation modulation of the mesophase, as a response to the total field $E_{SC} + E_{DC}$, would be relatively small. Such a reorientational effect, and thus the amplitude of the achievable refractive index modulation, would be considerably improved if the space charge field could control the mesophase switching process between two orientational states symmetrical around the tilt cone axis. In the ideal case, the largest possible amplitude of

the refractive index modulation could equal the spontaneous birefringence of the liquid crystal, if the material had a tilt angle $\theta = 45^\circ$. This result could be achieved in bistable devices, which were considered only very recently [11] in the context of PR FLCs research. Although the director in bulk FLCs adopts a helical structure, it was discovered [12] that by confining the material between closely-spaced glass plates (with a spacing smaller than the helical pitch), the natural helix could be suppressed. In the ideal case, the smectic layer planes are oriented perpendicular to the substrate plane and the resulting structure is called bookshelf geometry. The director can assume two stable positions where the substrate plane cuts the smectic cone, since there intrinsic conical constraint and surface constraint are simultaneously satisfied (see Fig. 1). These two positions are energetically equivalent: they are symmetrical around the cone axis and correspond to up and down polarization, respectively. If an electric field, above a certain threshold amplitude, is applied across this surface stabilized ferroelectric liquid crystal (SSFLC), a reorientation of the spontaneous polarization between $+P_s$ and $-P_s$ takes place, which is accompanied by a reorientation of the director on the tilt cone between the $+\theta$ and $-\theta$ states, since polarization and director orientations are coupled. If one managed to control the polarization switching via the photogenerated E_{SC} in a bistable SSFLCs, a higher refractive index modulation could be achieved, as a consequence of a director reorientation through an angle π around the layer normal.

In this article we report how the PR performance of SSFLCs was greatly improved by exploiting the PR mechanism to optically control

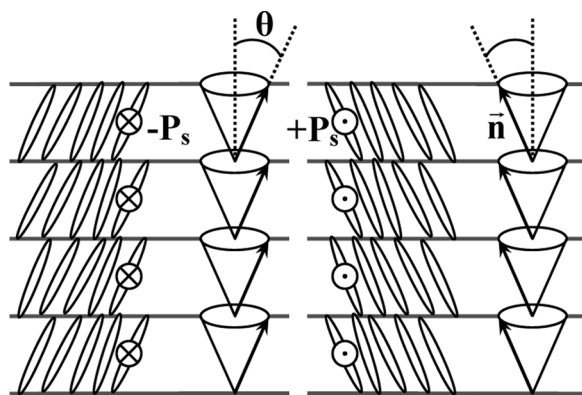


FIGURE 1 The two possible director orientations in a surface stabilized ferroelectric liquid crystal.

the mesophase switching between two stable orientational states. To achieve this goal, two main tasks had to be pursued: making photoconducting bistable SSFLC devices, and creating a suitable driving scheme, which enables the E_{SC} to control the switching process.

MATERIALS, SAMPLES PREPARATION AND EXPERIMENTAL METHODS

The FLC used in the present investigation is L-15278, an experimental fluorinated mixture from 3M. The choice of this liquid crystal was motivated essentially by its special layer thickness temperature dependence, which exhibits a minimal layer shrinkage through the transition from the orthogonal SmA^* phase to the tilted SmC^* phase. In this way, by choosing the suitable alignment agent, L-15278 offers the possibility of obtaining planar SmC^* alignment in the ideal bookshelf geometry, where layers simply remain normal or near normal to the cell substrates, avoiding the complications resulting from the presence of chevron structures, like the formation of zig-zag defects, that seriously degrade the alignment quality of electro-optic devices made of conventional FLCs.

In order to characterize the physical properties of L-15278, samples were prepared by placing the liquid crystal between two ITO-covered glass slides coated by an alignment agent (see Fig. 2). Two types of planar alignment agents were tested: Elvamide 8023 R and SiO_x . In the first case, on both glass slides a layer of Elvamide (a nylon multipolymer resin from DuPont) was spin-coated at 5000 rpm for 25 seconds from a 0.5 wt% methanol solution. After spin-coating, the excess of solvent was simply allowed to evaporate at room temperature. The nylon was then rubbed unidirectionally with a velvet cloth. In the second case, the oxide was heated in a vacuum chamber to evaporate and condense on the glass substrates. In both cases, the treated glass

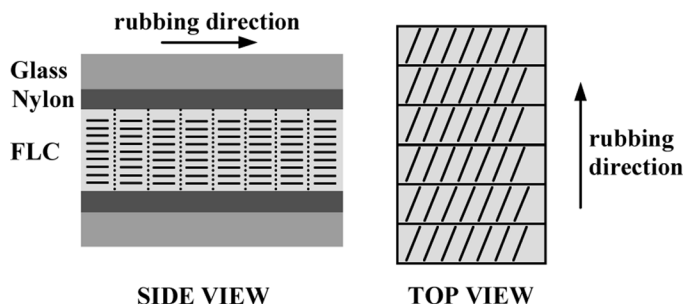


FIGURE 2 Schematic structure of the surface stabilized SmC^* device.

slides were then assembled into cells by using Norland 61 UV cured epoxy as a sealant. The cell thickness was controlled using spacers between 1.7 and 9 μm and finally checked by interferometric measurements. Once prepared, cells were filled by capillarity with L-15278 in the isotropic phase and very slowly (0.1°C/min) cooled down to room temperature, in the SmC* phase. L-15278 aligns very well on nylon, while with SiO_x many focal conics defects are observed.

The mesomorphic behaviour of L-15278 was investigated by optical microscopy and differential scanning calorimetry (DSC) and the observed transition temperatures are: Cr 18 SmC* 57.7 SmA* 96.0 I. Thus, this liquid crystal offers the advantage to be in the SmC* phase at room temperature, with no need of using a temperature controller during the experiments. The spontaneous polarization was measured by using the well known triangular waveform voltage method [13], where the current through the cell is monitored while simultaneously applying a triangular wave: a value of $P_S = 30.8 \text{ nC/cm}^2$ was obtained. In order to measure the tilt angle, a square wave of very low frequency (0.2–1 Hz) was applied, allowing a direct observation of the switching with a microscope, and the value $\theta = 22.5^\circ$ was obtained.

In properly aligned SmC* LCs, as in our case, the coupling between P_S and an applied electric field is described by a torque leading, in principle, to a microsecond response time [14]. Such behavior is also shown by L-15278: a switching time $\tau \sim 10 \mu\text{s}$ was measured under the application of a 10 V/ μm square wave of 1 kHz. To measure the pitch of L-15278, a planar 50 μm thick sample was prepared in order to minimize deformations of the SmC* helix due to the elastic interactions with the substrate, which would lead to pitch values larger than those of the undisturbed bulk material. In this way, a uniformly oriented structure with helix axes in the plane of the substrate was obtained: a unidirectional line pattern was observed in polarizing microscopy, and from the spatial periodicity of the pattern, an estimation of the SmC* pitch was obtained ($\sim 6 \mu\text{m}$).

As already outlined in the introduction, bistability is one crucial requirement and it was tested by applying positive and negative DC pulses while observing the optical response in polarized light microscopy. Two clearly different transmission states appeared in the optical transmission, as a function of the polarity of short DC electric pulses, confirming the excellent bistability of the prepared samples.

The following step was the preparation of bistable photosensitive devices. Two different approaches were used: in one case the photogeneration functionality was ensured by two photoconductive polymer layers placed between the liquid crystal and the substrates, while in a second case the FLC was made photosensitive by addition of a dopant.

The first approach has been never considered for PR FLC, but it gave good results with PR nematics [15] and spatial light modulators [16] containing bistable FLCs. The LC alignment is induced by a layer of a planar alignment agent spin-coated on the top of a photoconducting polymer. A schematic picture of the sample structure is depicted in Figure 3. Actually, in the attempt to obtain photoconducting bistable SSFLC devices, several combinations of photoconducting and alignment layers were tested (see in Table 1): sample types **a** and **b** are symmetrical with respect to both photoconducting and alignment layers, sample types **c** and **d** are symmetrical with respect to the photoconducting layer but not to the alignment layer and finally sample types **e** and **f** are completely asymmetric. The choice of the photoconductor fell on the well known poly(N-vinylcarbazole) (PVK) [17], which was used pure or in mixture with a plasticizer, 9-ethylcarbazole (ECZ). Light absorbance at the wavelength used (632.8 nm or 532 nm) was ensured by adding 2 wt% of 2,4,7-trinitro-9-fluorenone (TNF) [18], which forms a charge transfer complex with PVK. Photoconducting layers were prepared in a three steps procedure: PVK(98%):TNF(2%) or PVK(54%):ECZ(44%):TNF(2%) mixtures were first dissolved in chloroform, the resulting solution was cleaned on 0.5 μm filters and finally spin-coated for 50 s at 5000 rpm on ITO covered glass slides. In order to align the FLC, two kinds of planar alignment agents were tested, Elvamide and 3-glycidoxypropyl-trimethoxysilane (glymo). In particular, Elvamide was dissolved in methanol (0.5 wt%), while glymo in a water:isopropanol = 1:9 solution. Again, after filtration, the alignment agent solution was directly spin-coated for 25 s at 5000 rpm on the (PVK)/(PVK-ECZ)-TNF layer. One or both coated glass slides were unidirectionally rubbed with a velvet cloth and the thickness of the

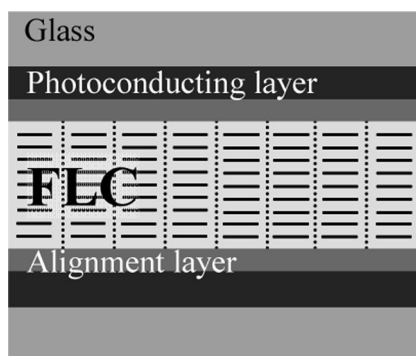


FIGURE 3 Schematic structure of samples **a–d** in Table 1.

TABLE 1 Structure of L-15278 Samples Containing Photoconducting Layers

Sample	Upper photoconducting layer	Upper alignment layer	Lower photoconducting layer	Lower alignment layer
a	PVK(98%)-TNF(2%)	Rubbed elvamide	PVK(98%)-TNF(2%)	Rubbed elvamide
b	PVK(54%)-ECZ(44%)-TNF(2%)	Rubbed elvamide	PVK(54%)-ECZ(44%)-TNF(2%)	Rubbed elvamide
c	PVK(54%)-ECZ(44%)-TNF(2%)	Rubbed elvamide	PVK(54%)-ECZ(44%)-TNF(2%)	Glymo
d	PVK(54%)-ECZ(44%)-TNF(2%)	Rubbed elvamide	PVK(54%)-ECZ(44%)-TNF(2%)	Unrubbed elvamide
e	PVK(54%)-ECZ(44%)-TNF(2%)	Rubbed elvamide	–	Unrubbed elvamide
f	PVK(54%)-ECZ(44%)-TNF(2%)	Rubbed elvamide	–	Glymo

liquid crystal was controlled with 1.7 μm , 3 μm or 5 μm spacers. Finally, cells prepared by using the procedure described above were filled by capillarity with L-15278 in the isotropic phase and slowly cooled at 0.1°C/min to room temperature in order to obtain a good orientation of the director. Bistability of samples was tested and only devices of type **a** turned out to be interesting for our purposes. They were not bistable in the usual sense, since, by applying short (~ 1 ms) DC electric pulses of both polarities, their optical transmission shows two just slightly different transmission states (Fig. 4a). But if the length of the pulse is increased, bistability is obtained, probably due to the onset of a depolarization electric field, which develops during the application

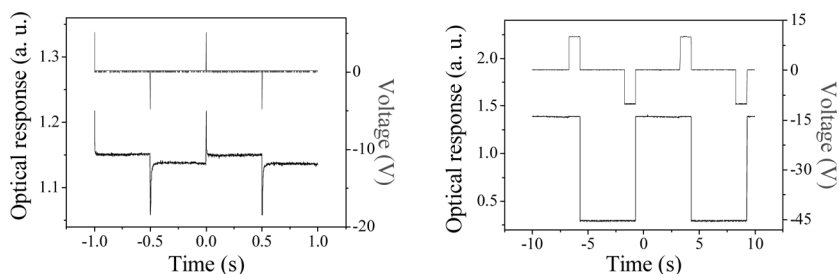


FIGURE 4 (a) Applied voltage (grey) and optical response (black) for a 5 μm thick sample of type **a** (see Table 1). The pulse length was 1 ms. (b) Optical response (black) for the same sample under ± 10 V DC pulses (grey) 1 s long. The FLC switches in the other stable state exactly at the end of the pulse ($V = 0$), revealing the existence of a depolarization field.

of the pulse (Fig. 4b). That such a field exists was also confirmed by the observation of FLC switching when applied potentials of 10 V are switched off, both in the dark and under illumination. Unfortunately, all the other samples (type **b–f** in Table 1) were either not bistable at all or, in some cases, monostable (type **c** and **f** samples).

As already anticipated above, the second approach used in the attempt to prepare bistable photosensitive SSFLC devices consisted in doping L-15278 with 0.2 wt% fullerene C₇₀. This approach is not a novelty since in almost all the reported investigations about PR FLCs, LCs were doped in order to get photoconductivity, even though never with fullerenes, which instead have been widely used as photosensitizers [19] for both PR nematics and polymers. A 0.2 wt% solution of C₇₀ (Aldrich) in L-15278 was obtained by dissolving both substances in chloroform and by evaporating the solvent. Samples were then prepared by filling 3 to 5 μm thick cells treated with elvamide (the cell preparation procedure has been already described at the beginning of the paragraph) with the doped L-15278 in the isotropic phase ($T = 100^\circ\text{C}$) and good alignment of the mesophase was obtained again by cooling to room temperature at a speed of $0.1^\circ\text{C}/\text{min}$. Cells filled with doped L-15278 look very similar to those filled with the pure FLC, except for the fact that they exhibit a slightly worse alignment, due to a small increase in the number of defects. After doping, samples still exhibit high optical clarity (total losses were estimated to be $\alpha \sim 60 \text{ cm}^{-1}$ at $\lambda = 532 \text{ nm}$) and the physical properties of the LC are left almost unchanged by the introduction of C₇₀.

Bistability of these samples was assessed by using the method already described above and the optical transmission between crossed polarizers shows the existence of two homogeneous states which remain perfectly stable even after the field is removed (see Fig. 5). Finally, the photoconducting nature of the doped SSFLC devices was confirmed by measuring the current flowing through samples, with and without light exposure (a Keithley 6517 A electrometer was used). A photoconductivity $\sigma_p = 5.3 \cdot 10^{-11} \Omega^{-1} \text{ cm}^{-1}$ was obtained at an applied field $E = 0.3 \text{ V} \mu\text{m}^{-1}$ by irradiating with 532 nm light having a power density $I = 0.4 \text{ W cm}^{-2}$ (the measured dark conductivity was instead $\sigma = 7.3 \cdot 10^{-13} \Omega^{-1} \text{ cm}^{-1}$).

OPTICAL CONTROL OF ORIENTATIONAL BISTABILITY IN FLC PLACED BETWEEN PHOTOCONDUCTIVE POLYMER LAYERS

Even if the bistability exhibited by type **a** samples was not the usual one, they were used in the attempt to optically control the polarization

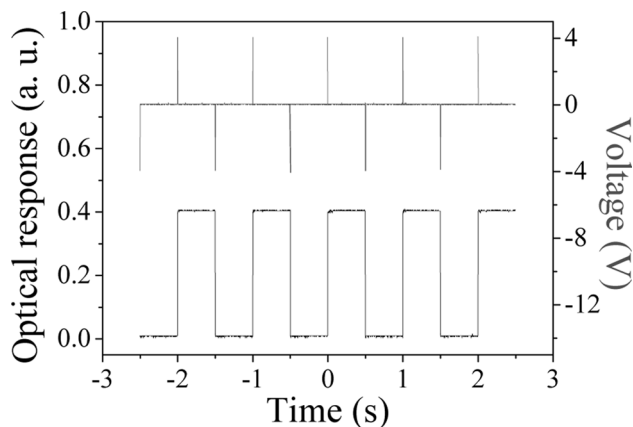


FIGURE 5 Optical response (black) through crossed polarizers to 1 ms long applied voltages (grey) of opposite signs of a $4.8\ \mu\text{m}$ thick sample of C_{70} doped L-15278.

switching via a PR mechanism. To achieve this goal, two tasks had to be pursued: the first was the photogeneration of E_{SC} , which, as usual with organic materials, could be established only by applying a sufficiently strong external electric field during the exposition to a non-uniform illumination. In addition the amplitude of such externally applied field had to be tuned in order to enable the spatially modulated E_{SC} to control the mesophase switching (E_{SC} is assumed to be lower than the switching threshold of the FLC).

The driving scheme (I), that gave the best results with samples of type **a**, is shown in Figure 6. It consists of a relatively strong external electric field (E_{AP}) applied for a time T_{A} , which is then lowered to a smaller value for a time T_{B} . Since the applied field is higher than the FLC switching threshold, during T_{A} the director is oriented along one of its two stable positions, and E_{SC} , together with a depolarization field (E_{dep}), develops. In particular, E_{SC} forms on the surfaces of the liquid crystal, since L-15278 is sandwiched between two photoconducting layers. When E_{AP} is lowered, its value is adjusted in such a way that the sum $E_1 = E_{\text{AP}} + E_{\text{DEP}}$ is slightly below the threshold necessary to switch the liquid crystal director to the other of its two stable positions. Thus, considering the simultaneous presence of both E_1 and of E_{SC} , in some regions of the sample E_{SC} and E_1 will point in opposite directions and the total field $E_{\text{TOT}} = E_1 + E_{\text{SC}}$ will be lower than the threshold required to switch the FLC, which will remain in its initial state. In other regions, E_1 and E_{SC} will have the same sign and E_{TOT}

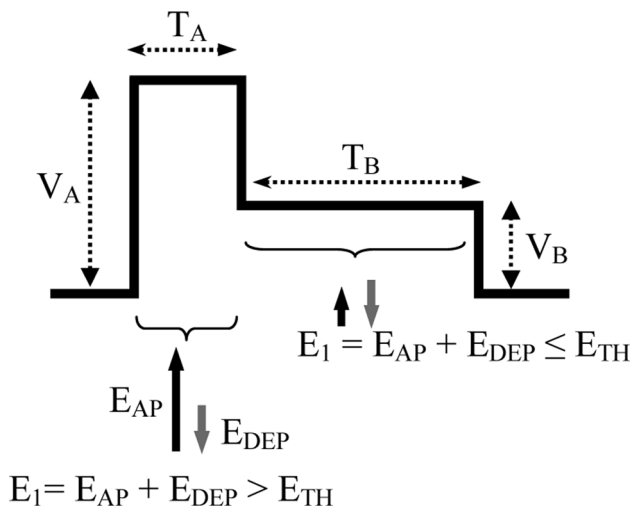


FIGURE 6 Driving scheme I used to control the polarization switching in samples containing photoconducting layers. During T_A the field E_1 is higher than the switching threshold, while during T_B is just below.

will be strong enough to switch the mesophase to the other stable state.

The writing light source was either a He-Ne laser ($\lambda = 632.8$ nm) or a diode pumped solid state laser ($\lambda = 532$ nm). The laser beam was divided in two beams of approximatively equal intensity ($I \sim 3.5$ mW) interfering on the sample. The sample normal was tilted by 60° with respect to the beams bisector and the rubbing direction of the Elva-mide layer was in the p-plane (defined by the light beams and the sample normal). The beams polarization was set to $+22.5^\circ$ with respect to the p-plane. A schematic picture of the experimental set-up is shown

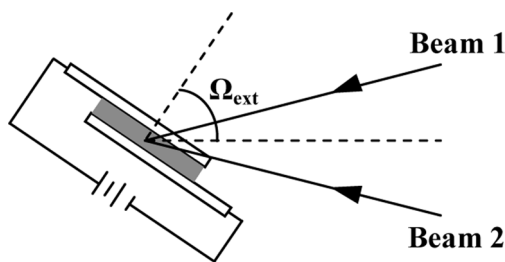


FIGURE 7 Experimental geometry used to generate PR gratings in L-15278 sample cells.

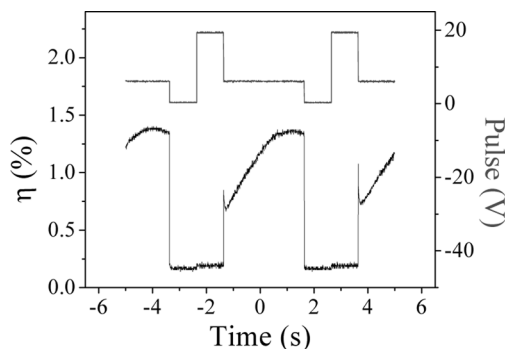


FIGURE 8 Applied voltage (grey) and first order diffraction efficiency (black) as a function of time for a type **a** sample with a thickness of $5\ \mu\text{m}$. The driving scheme parameters were: $V_A = 20$, $T_A = 1\ \text{s}$, $V_B = 6\ \text{V}$, $T_B = 3\ \text{s}$.

in Figure 7. In such experimental conditions and by applying the driving scheme I, up to two diffraction orders were observed, giving evidence of the grating formation. In particular, the resulting gratings were characterized by measuring the first order diffraction efficiency, η , defined as the ratio between the intensities of the diffracted beam and the transmitted beam without the grating. For a spatial periodicity of the interference pattern $\Lambda = 20\ \mu\text{m}$ and at $T = 25\ ^\circ\text{C}$, typically $\eta \sim 1.2\%$ (see Fig. 8). The first order diffraction rise time was also measured, obtaining a value close to 2 ms. However, in two-beam coupling experiments it was never possible to detect an energy transfer between the writing beams, essentially because of the poor quality of the gratings, caused probably by the imperfect alignment of the FLC. Moreover, significant optical losses were induced by the high scattering of the samples. Since the presence of a double layer on the cell surfaces was soon recognized as the origin of all these problems, in order to improve the alignment and the bistability of our SSFLC devices, the “doping approach” in sample preparation was taken under consideration.

OPTICAL CONTROL OF ORIENTATIONAL BISTABILITY IN DOPED SSFLCS

In this case the formation of E_{SC} does not occur on the surfaces confining the LC, but in its bulk, and the absence of multi layers prevents the appearance of depolarization fields. Moreover, doped samples exhibit good alignment and perfect bistability.

In order to write PR gratings, several types of driving schemes were tested, but the best results were obtained by first applying an electric field E_A for a time T_A (while providing the non-uniform illumination), followed by a field E_B , of opposite sign, lower than the switching threshold (driving scheme II, shown in Fig. 9). As already outlined, E_A promotes the E_{SC} formation while E_B “helps” E_{SC} in the switching process: only in the regions of the sample where the total field $E_{SC} + E_B$ is higher than the threshold, the FLC will switch.

The experimental set-up used to induce the PR gratings formation was very similar to that adopted with layered SSFLC samples: the driving voltage scheme described above was applied to samples exposed to the interference pattern of two 532 nm laser beams having the same polarization and intensity $I \sim 2.3 \text{ mW}$ (the overlapping region was $S \sim 1 \cdot 10^{-2} \text{ cm}^2$). The sample normal was also in this case tilted by 60° with respect to the beams bisector and the rubbing direction lay in the p-plane. With this geometry, E_{SC} would have one component normal to the layers and one component within the layers, in the same direction of the applied field. The beams polarization was set to $+22.5^\circ$ with respect to the p-plane and the spatial periodicity of the interference pattern, Λ , ranged between 2 and $40 \mu\text{m}$.

By applying the driving scheme II, the formation of good quality gratings was obtained: in the best experimental conditions up to eight diffraction orders were observed. The existence of a modulation of the LC refractive index was also confirmed by observing samples subjected to the writing process in polarizing microscopy: a striped texture was visible, with the director alternatively oriented along

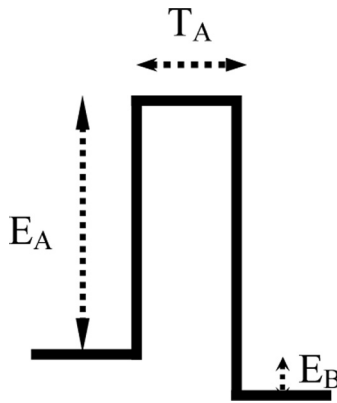


FIGURE 9 Driving scheme II used to control the polarization switching in doped samples.

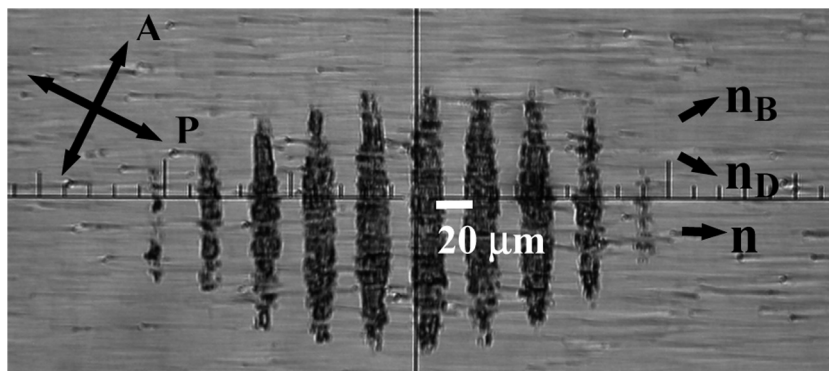


FIGURE 10 Optical microscope picture of a C₇₀ doped L-15278 sample, placed between crossed polarizers, after applying the driving pulse. The period of the interference pattern was $\Lambda = 40 \mu\text{m}$. n , n_B and n_D indicate the orientations of the layer normal and of the director in the bright and dark regions, respectively.

either of its two stable positions (see Fig. 10). Given the bistability of SSFLC doped samples, once written, gratings are stable for at least one year, and they can only be erased by applying an electric field above the switching threshold, making the read-out process completely not destructive.

In order to characterize and optimize the grating formation process in our bistable SSFLC devices, a set of η measurements were performed at $\Lambda = 5 \mu\text{m}$ as a function of the three driving scheme parameters: E_A , T_A , E_B . η increases with increasing E_A until $E_A \sim 2.1 \text{ V}/\mu\text{m}$, where η settles at 2.3% (see Fig. 11). This value of E_A is probably the one required to maximize the photogeneration and drift mobility processes and the application of a stronger field would not further improve the amplitude of E_{SC} . The dependence of η on T_A shows instead a different pattern: at first η increases with T_A so that it reaches a maximum at 500 ms, and then it decreases (see Fig. 12). But since the “increasing” part of the pattern is very steep, good efficiencies are also obtained with $T_1 \sim 150\text{--}200 \text{ ms}$. From the dependence of η on E_B , other interesting information can be obtained. As shown in Figure 13, even at $E_B = 0$, a grating forms with quite high efficiency (3.5%), suggesting that E_{SC} can be intense enough to control the mesophase switching. By increasing E_B , η at first reaches a maximum (4.7% at $0.05 \text{ V}/\mu\text{m}$) and then goes to zero since the applied field is so intense that the liquid crystal is uniformly switched. Considering all these data, the best combination of parameters, which maximize η , could be obtained: $E_A = 2.1 \text{ V}/\mu\text{m}$,

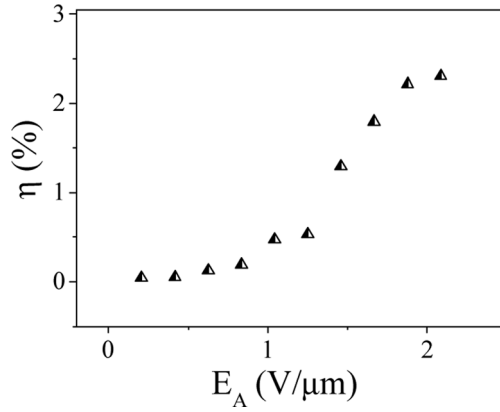


FIGURE 11 First order diffraction efficiency as a function of the intensity of the applied field E_A with $\Lambda = 5 \mu\text{m}$, $E_B = -0.05 \text{ V}/\mu\text{m}$ and $T_A = 500 \text{ ms}$.

$T_A = 500 \text{ ms}$, $E_B = -0.05 \text{ V}/\mu\text{m}$. The maximum resolution of these gratings was determined by measuring the dependence of η on Λ . Of course, the efficiency decreases with Λ , going from 10.1% at $\Lambda = 40 \mu\text{m}$ to 0.5% at $\Lambda = 2 \mu\text{m}$ (see Fig. 14).

Once established that refractive index gratings with good efficiencies could be written in properly driven doped samples of L-15278, the subsequent step consisted in performing experiments to prove their PR nature: two-beam coupling [5] and direct phase shift measurements [20,21]. The two-beam coupling technique measures

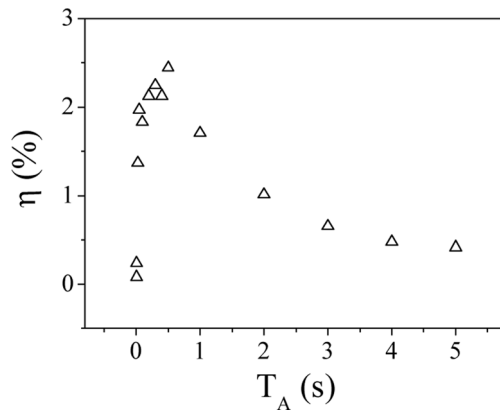


FIGURE 12 First order diffraction efficiency as a function of T_A with $\Lambda = 5 \mu\text{m}$, $E_A = 2.1 \text{ V}/\mu\text{m}$ and $E_B = -0.05 \text{ V}/\mu\text{m}$.

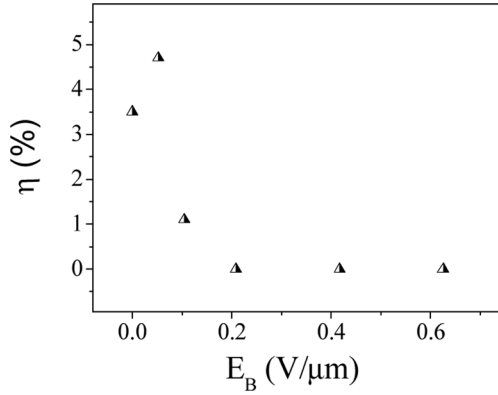


FIGURE 13 First order diffraction efficiency as a function of the intensity of the applied field E_B with $\Lambda = 10 \mu\text{m}$, $E_A = 2.1 \text{ V}/\mu\text{m}$ and $T_A = 500 \text{ ms}$.

possible energy exchanges between the two writing beams (the experimental set-up is the same of that described for η measurements, except for the fact that this time the intensities of both writing beams are monitored), giving information about the grating phase. The energy transfer is only allowed if the material has a non-local response, meaning that the light distribution inducing the grating and the grating itself are phase shifted. This non-local response is uniquely achieved in PR materials, and thus two-beam coupling is usually a direct evidence of photorefractivity, at least in the Bragg diffraction regime.

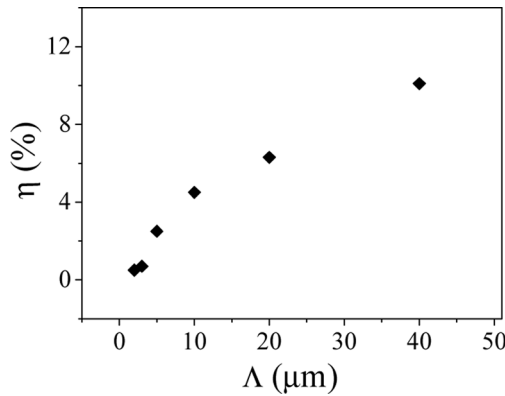


FIGURE 14 First order diffraction efficiency as a function of Λ , obtained for $E_A = 2.1 \text{ V}/\mu\text{m}$, $T_A = 500 \text{ ms}$ and $E_B = -0.05 \text{ V}/\mu\text{m}$.

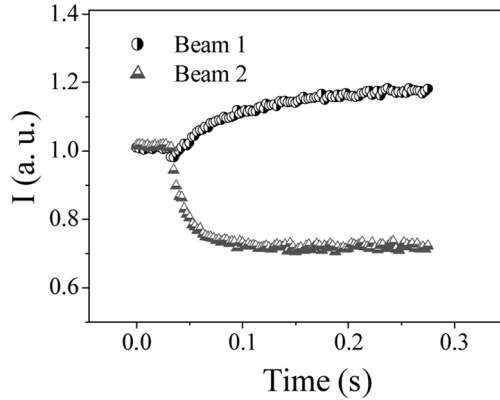


FIGURE 15 Intensities of the two writing beams during a two-beam coupling experiment on a $4.8\text{ }\mu\text{m}$ thick sample of C_{70} doped L-15278. The grating formation begins at $t \sim 32\text{ ms}$ where the applied field is changed from $E_A (= 2.1\text{ V}/\mu\text{m})$ to $E_B (= -0.05\text{ V}/\mu\text{m})$.

Two-beam coupling experiments were performed on C_{70} doped L-15278 samples, and a typical result, shown in Figure 15, reveals a strong energy exchange between the writing beams with a beam coupling ratio [22] $\gamma_1 = I_1 (I_2 \neq 0) / I_1 (I_2 = 0) = 1.18$, where I_1 and I_2 are the intensities of the two beams. This value of γ is the highest ever measured in PR FLCs so far [11]. Moreover, from these data a grating formation time $\tau \sim 40\text{ ms}$ can be also evaluated: if we consider that high efficiencies are obtained even with T_A of $150\text{--}200\text{ ms}$, the total time required for writing a grating with high efficiency is roughly 200 ms .

The gratings obtained in doped L-15278 samples fall in the Raman-Nath regime, where multiple diffraction orders are allowed and energy exchanges between the writing beams cannot necessarily be brought back to the existence of a phase shift [23]. To establish the PR nature of doped SSFLC samples without doubt, a direct measurement of the phase shift between light pattern and refractive index grating became necessary. Immediately after the writing process, the intensities of both writing beams were monitored while the sample was mechanically translated by a precision translator (OptoMikeTM from Opto-Sigma), driven by a DC motor with a $1\text{ }\mu\text{m}$ resolution, along the direction of the grating wavevector at a velocity $v \sim 100\text{ }\mu\text{m/s}$, which is much faster than the response time of the material to the spatially varying illumination. This process changes the relative phase between the intensity pattern and the grating, resulting in intensity oscillations in both the transmitted beams, which are used to determine

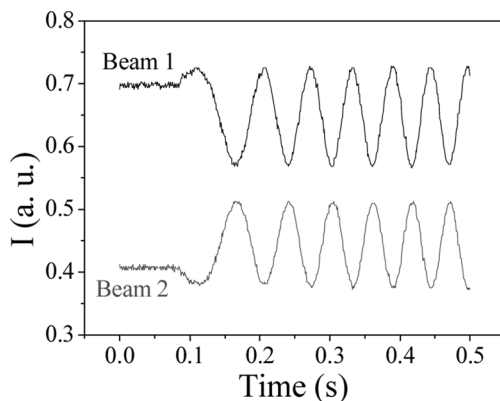


FIGURE 16 Intensities of the two writing beams monitored after the grating build-up. At $t \sim 80$ ms, the sample is translated at a constant velocity $v \sim 100 \mu\text{m/s}$ along the direction of the grating wavevector.

the phase shift Φ . In our case, $\Phi = 40^\circ \pm 10^\circ$ was measured (see Fig. 16), confirming that the stable refractive index gratings which can be easily written, erased and rewritten in our photoconductive and bistable SSFLC devices have a photorefractive nature.

CONCLUSIONS

In this article the first attempts towards an optical control of the polarization switching in bistable SSFLC devices via a photorefractive (PR) mechanism are reported. To accomplish this goal, two different approaches were used: in the first case the space-charge field was generated on the surfaces of the SSFLC device, by sandwiching the FLC between two photoconducting layers, while in the second case it was generated in the mesophase bulk by doping. In the first case the formation of stable gratings was obtained, but it was not possible to measure any energy exchange between the writing beams. In doped samples, a substantial improvement of alignment and bistability was obtained, allowing the achievement of stable gratings which are easily erasable and rewritable. To confirm the PR origin of such gratings, both two-beam coupling experiments and direct phase shift measurements were performed. A beam coupling ratio $\gamma_1 = 1.18$ and a phase shift $\Phi = 40^\circ \pm 10^\circ$ were measured, demonstrating that the mesophase switching in our bistable SSFLC devices was effectively controlled by the photogenerated E_{SC} through a PR mechanism.

REFERENCES

- [1] Yeh, P. (1993). *Introduction to Photorefractive Nonlinear Optics*, John Wiley & Sons: New York, USA.
- [2] Huignard, J. P. & Herriau, J. P. (1977). *Appl. Opt.*, **16**, 1807.
- [3] Owechko, Y. (1989). *IEEE J. Quantum Electron.*, **25**, 619.
- [4] Günter, P. (2000). *Nonlinear Optical Effects and Materials*, Springer-Verlag: Berlin, Germany.
- [5] Solymar, L., Webb, D. J., & Grunnet-Jepsen, A. (1996). *The Physics and Applications of Photorefractive Materials*, Oxford University Press: Oxford, UK.
- [6] Rudenko, E. V. & Sukhov, A. V. (1994). *JETP Lett.*, **59**, 142.
- [7] Khoo, I. C., Li, H., & Liang, Y. (1994). *Opt. Lett.*, **19**, 1723.
- [8] Wiederrecht, G. P., Yoon, B. A., & Wasielewski, M. R. (2000). *Adv. Mater.*, **12**, 1533.
- [9] Termine, R., De Simone, B. C., & Golemme, A. (2001). *Appl. Phys. Lett.*, **78**, 688.
- [10] Termine, R. & Golemme, A. (2002). *J. Phys. Chem.*, **106**, 4105.
- [11] Talarico, M. & Golemme, A. (2006). *Nature Materials*, **5**, 185.
- [12] Clark, N. A. & Lagerwall, S. T. (1980). *Appl. Phys. Lett.*, **36**, 899.
- [13] Miyasato, K., Abe, S., Takezoe, H., Fukuda, A., & Kuze, E. (1983). *Jpn. J. Appl. Phys. Lett.*, **22**, L661.
- [14] Lagerwall, S. T. (1999). *Ferroelectric and Antiferroelectric Liquid Crystals*, Wiley-VCH: Weinheim, Germany.
- [15] Ono, H. & Kawatsuki, N. (1998). *Opt. Commun.*, **147**, 237.
- [16] Kurosawa, T. & Fukushima, S. (1992). *Optical and Quantum Electronics*, **24**, 1151.
- [17] Mecher, E., Gallego-Gomez, F., Tillmann, H., Horhold, H. H., Hummelen, J. C., & Meerholz, K. (2002). *Nature*, **418**, 959.
- [18] Kippelen, B., Marder, S. R., Hendrickx, E., Maldonado, J. L., Guillemet, G., Volodin, B. L., Steele, D. D., Enami, Y., Sandalphon, Yao, Y. J., Wang, J. F., Rockel, H., Erskine, L., & Peyghambarian, N. (1998). *Science*, **279**, 54.
- [19] Khoo, I. C., Guenther, B. D., Wood, M. V., Chen, P., & Shih, M. Y. (1997). *Opt. Lett.*, **22**, 1229.
- [20] Walsh, C. A. & Moerner, W. E. (1992). *J. Opt. Soc. Am. B*, **9**, 1642.
- [21] Grunnet-Jepsen, A., Thompson, C. L., & Moerner, W. E. (1997). *Optics Letters*, **22**, 874.
- [22] Ostroverkhova, O. & Moerner, W. E. (2004). *Chem. Rev.*, **104**, 3267.
- [23] Sanchez, F., Kayoun, P. H., & Huignard, J. P. (1988). *J. Appl. Phys.*, **64**, 26.